Digital Object Identifier 10.1109/ICIT.2019.8755238

2019 IEEE International Conference on Industrial Technology (ICIT)

Peak Current Control and Feed-Forward Compensation for the DAB Converter

Nimrod Vazquez

Marco Liserre

Suggested Citation

N. Vazquez and M. Liserre, "Peak Current Control and Feed-Forward Compensation for the DAB Converter," 2019 IEEE International Conference on Industrial Technology (ICIT), Melbourne, VIC, Australia, 2019.

Peak Current Control and Feed-Forward Compensation for the DAB Converter

Nimrod Vazquez
Electronics department
Tecnologico Nacional de Mexico
/Instituto Tecnologico de Celaya
Celaya, Mexico
n.vazquez@ieee.org

Marco Liserre
Chair of Power Electronics
University of Kiel
Kiel, Germany
ml@tf.uni-kiel.de

***Abstract*—This paper presents a double band peak current control for the DAB converter that permits to avoid the risk of transformer saturation. Additionally, feed-forward compensation is employed to achieve a fast transient response under load variations. The proposal is described, analyzed, and numerically simulated.**

Keywords— DAB Converter, Peak current control, Transformer saturation.

I. INTRODUCTION

Double active bridge (DAB) converter is one of the most employed power stages for different applications, like the solid-state transformers [1]-[7], multiple input converters [8]-[12], and more applications [13]-[14]. This converter provides isolation between the input and output, by employing a high-frequency transformer (Fig. 1), and then reducing volume and space. Additionally, the input voltage, output voltage, and power level may be selected by design, this is why the converter is suitable for many applications.

The DAB converter have been studied extensively in different aspects, the modulations techniques are focusing on reducing losses at different operating modes [15]-[18]. In [15] an algorithm to control the power flow, but mainly to minimize the total power losses of the DAB converter is proposed, based on the modulation. A similar method in [16] is proposed, that is focused on assuring soft-switching in the whole range of power, by changing the modulation technique. Different modes of operations are proposed in [17] to increase the efficiency, the burst mode and frequency change are considered.

Another important aspect in isolated converters is transformer saturation. The importance of avoiding it is because of results in overcurrent troubles that might incur in switches damage or in the best way of triggering current protection that implies to shut down the converter [19].

This work was supported by the European Research Council under the European Union's Seventh Framework Programme (FP/2007- 2013)/ERC Grant Agreement 616344 HEART—the Highly Efficient And Reliable smart Transformer.

Also this work was sponsored by CONACyT under project No. 291626 (I0000/727/2017)

Regarding preventing transformer saturation for DAB converters, different works have been proposed [19]-[22].

In [19] is proposed, for a type of DAB converter, an extra control loop to eliminate the possible DC offset at the transformer, it is measured the transformer current at the primary and secondary windings, additionally to other variables. A control loop is employed for both power bridges. This scheme does not assure a fast dynamic response, and also multiple variables are measured.

In [20]-[21] are proposed predictive controllers, employing a peak current control. These schemes permit to predict the displacement phase of the DAB converter for the desired peak current reference, the transformer saturation might be avoided, but not proofs of that were shown. In [22] a similar controller is employed, but to operate in a bidirectional way. Despite the before mentioned, feed-forward compensation is not included, resulting in a low response if the output voltage is controlled since the current reference depends on the voltage loop.

Other control schemes have been proposed to achieve a good dynamic response and to operate in a bidirectional way, but they do not consider peak current control [23]-[28]. In [23] is proposed a feed-forward compensator for the phase lag control. In [24] another type of feed-forward compensation is employed based on average current control. An output current estimator and a feed-forward compensator are proposed in [25], the control is based on the average output current.

In this paper is proposed a double-band peak current control to avoid transformer saturation for the DAB converter, but also a feed-forward compensation is considered for a fast

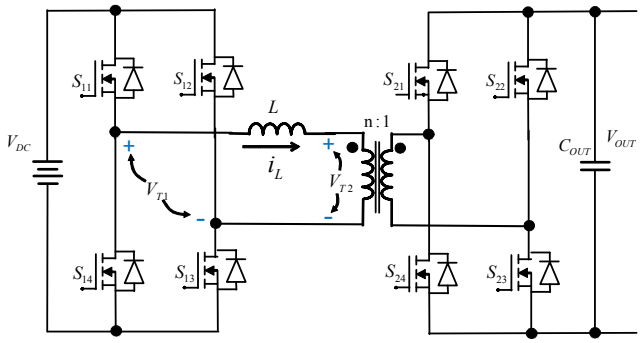

Fig. 1. Double Active Bridge (DAB) Converter

dynamic response when the output voltage regulation is required. The system is described, analyzed, modeled, designed, and numerically simulated to demonstrate the performance of the proposal.

II. Double Active Bridge Converter

The DAB converter is shown in Fig. 1, as it can be observed it is composed of two full-bridge stages, a transformer, and additionally, an inductor in series may be employed in combination with the inductive parasitic element of the transformer. The simplified circuit usually considered for this converter is the shown in Fig. 2(a) [23], where two square voltage sources are considered plus the inductive element.

A. Steady state analysis

The steady-state waveforms of the DAB converter for the selected operating mode are shown in Fig. 2(b), it can be observed the voltage sources with its phase displacement, but also the inductor current. When the current reaches the valley and the peak value, the transition of the voltage V_2 is made.

Considering these waveforms, the converter is analyzed. Then, the inductor current is:

$$i_L(\theta)=\begin{cases}\dfrac{V_1+V_2}{\omega L}\theta-\mathrm{I}_0 & 0\le\theta\le\delta\\ \dfrac{V_1-V_2}{\omega L}\theta+\dfrac{V_1+V_2}{\omega L}\delta-\mathrm{I}_0 & 0\le\theta\le\pi-\delta\end{cases} \quad (1)$$

where: ω is the switching angular frequency,

I_0 is the initial current,

L is the inductance of the topology.

The other semi-cycle of the inductor current is omitted since it is symmetrical, due to the ac operation. Notice that the vertical axis was shifted to determine the second equation, this was made for simplification purposes on the analysis.

Due to the half-wave symmetry, the value of the inductor current at π–δ is determined by:

$$i_L(\pi-\delta)=\frac{V_1-V_2}{\omega L}(\pi-\delta)+\frac{V_1+V_2}{\omega L}\delta-\mathrm{I}_0=\mathrm{I}_0 \quad (2)$$

Then, the initial current value may be determined from (2), and it is given by:

$$\mathrm{I}_0=\frac{1}{2\omega L}\left[V_1(\pi)-V_2(\pi-2\delta)\right] \quad (3)$$

The peak current of the inductor, then, it is determined by the first term of (1) and (3), but solving at δ, resulting:

$$i_P=\frac{1}{2\omega L}\left[V_1(2\delta-\pi)+V_2(\pi)\right] \quad (4)$$

The valley of the inductor current is then the negative value of (4).

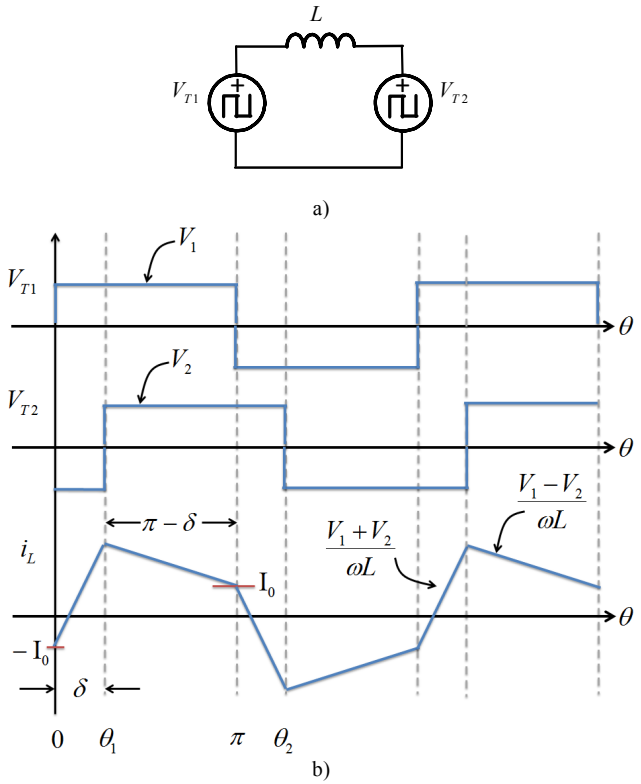

Fig. 2. DAB Converter: a) Simplified circuit, b) Waveforms

The power can be determined by considering just the first semi-cycle, that is:

$$P=\frac{1}{\pi}\int_0^{\pi}V_1 i_L\,d\theta \quad (5)$$

Then considering the intervals of the current, the equation (5) becomes in:

$$P=\frac{1}{\pi}\left[\int_0^{\delta}(V_1 i_L)d\theta+\int_0^{\pi-\delta}(V_1 i_L)d\theta\right] \quad (6)$$

And considering (1), (3), (6), and simplifying is obtained:

$$P=\frac{V_1V_2}{\omega L}\delta\left(1-\frac{\delta}{\pi}\right) \quad (7)$$

III. Proposed Controller

The block diagram of the proposed controller is illustrated in Fig. 3. As it can be observed, it is composed by a voltage compensator, the feed-forward compensation, the double band peak current controller, and a combinational logic circuitry. Each block is described in detail in the following sections.

A. Voltage compensator

The voltage compensator is used to determine the value of the peak current that assures the proper voltage regulation. When the feed-forward compensator is used, only a proportional controller (K_P) may be considered in this case.

In case that the feed-forward is not employed, a PI compensator is recommended, or at least an integrator term,

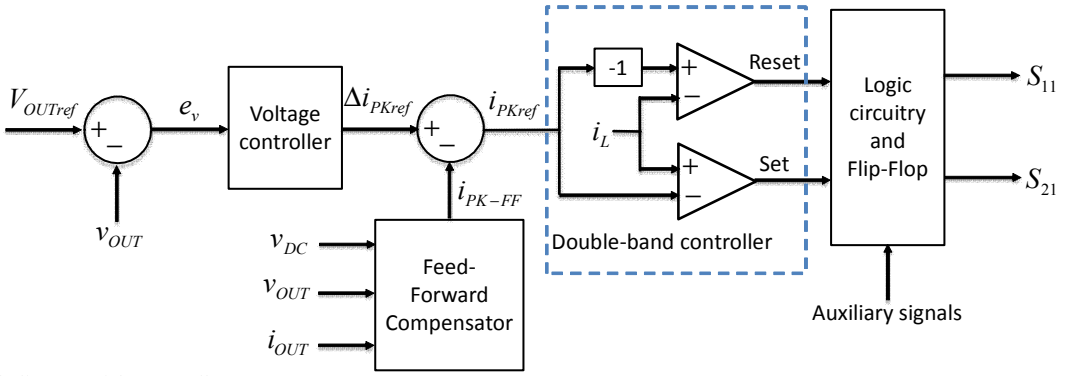

Fig. 3. Block diagram of the controller

because a significant steady-state error will appear if not, but also the dynamic response will be deteriorated. Then, to assure a fast dynamic response the feed-forward compensator is recommended.

B. *Feed-forward compensator*

The feed-forward compensator is used to assure a fast response under input/output variations, the operating point is determined and added to the voltage compensator output. This means that ideally at steady-state, the output of the voltage compensator is zero, because the feed-forward loop determines the operating point, and therefore only acts when it is required.

In our case, the operating point to be determined is the peak of the inductor current, and this is determined by (4). This means that the input voltage, output voltage, the system parameters, but also the displacement angle are required to get this peak current. The value of this angle is obtained from (7), resulting:

$$\delta = \frac{\pi}{2} \pm \pi \sqrt{\frac{1}{4} - \frac{P}{a}} \tag{8}$$

where: P is the output power,

$$a = \frac{V_1 V_2}{2 f_s L}.$$

The output power is determined by measuring the output voltage and current, and "a" depends on the known variables. The sign considered in (8) is the negative, since it is operated with a displacement phase lower than π/2. Then, considering (4) and (8), the peak current of the inductor is estimated and used as feed-forward compensation (Fig. 4(a)). Additionally, a first order low pass-band filter was employed to reduce the high-frequency noise at the output.

C. *Double-band peak current controller*

The peak current reference obtained from adding the voltage compensator output and the feed-forward stage output is used as the set point for the controller. The positive and negative values of this reference are considered for control purposes (hysteresis band), as illustrated in Fig. 4(b).

When the inductor current reaches the positive value of the band, the output voltage of VT2 is turned to the positive value. However, when the inductor current reaches the negative band, the output voltage of VT2 is turned to the negative value.

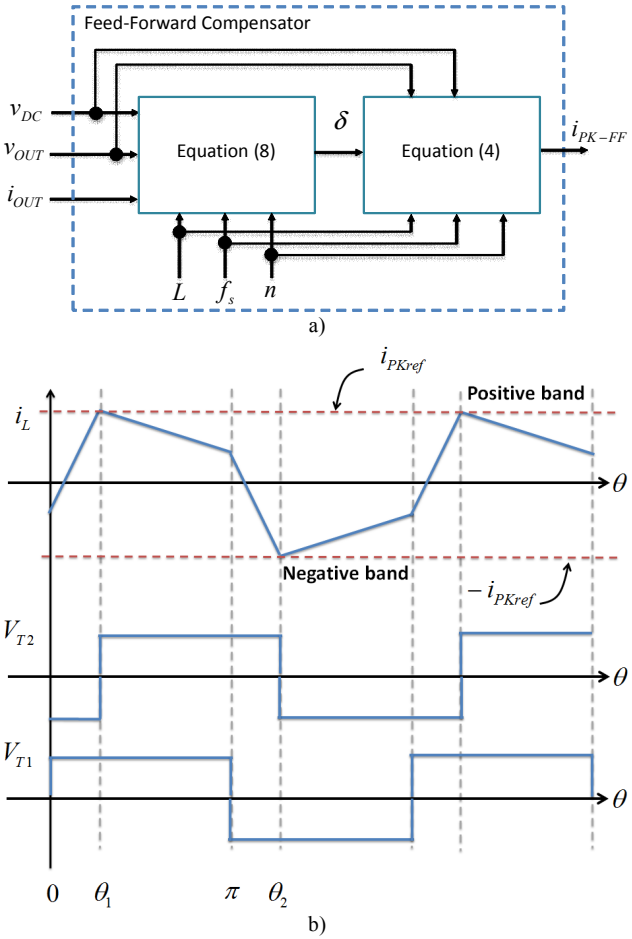

Fig. 4. Proposed controller: a) Feed-forward compensator, b) Waveforms of the double band controller

When the current is in between the two bands the actual state of VT2 is maintained.

To assure this operation a flip-flop SR is employed, that is triggered by the double band comparators.

D. *Logic circuitry and flip-flop*

The last stage is a logic circuitry, and it is employed to assure the operation of the proposal. This circuit permits to fix the switching frequency, but also it determines the range of the displacement phase angle. Also includes the Flip-Flop RS.

Since the converters are operated in a bipolar manner only S_{11} and S_{21} are obtained, since the other control signals of the switches are automatically determined by this operation.

IV. Simulation Results

The converter was designed and numerically simulated. The software employed is PSIM®. The parameters are summarized in Table I. In order to evaluate the performance of the system, different tests were carried out. First the steady state is addressed; second, a load variation is made; and finally, the performance of the system to avoid the transformer saturation is presented.

A. Steady state operation

The results for the converter operating at steady state is shown in Fig. 5. The tests were performed for around 95% of the nominal output power, then a resistive load of 24Ω was employed. In Fig. 5(a), the waveforms of V_{T1}, V_{T2}, and the primary current of the transformer or inductor current are shown. As it can be observed the converter is effectively working in the boosting mode since V_{T2} is higher than V_{T1}, but also the inductor current is being discharged during π–δ. That correspondence with the theory. And finally in Fig. 5(b), the output voltage ripple is shown and contrasted with other signals.

B. Load variation

A load variation was performed in order to evaluate the performance of the controller (Fig. 6). The load was changed from 24Ω to 48Ω at 0.5 ms. In Fig. 6(a) are shown the output voltage, the inductor current, the current obtained from the feed-forward compensator, but also the output current. The settling time is less than 15ms, and the maximum overshoot

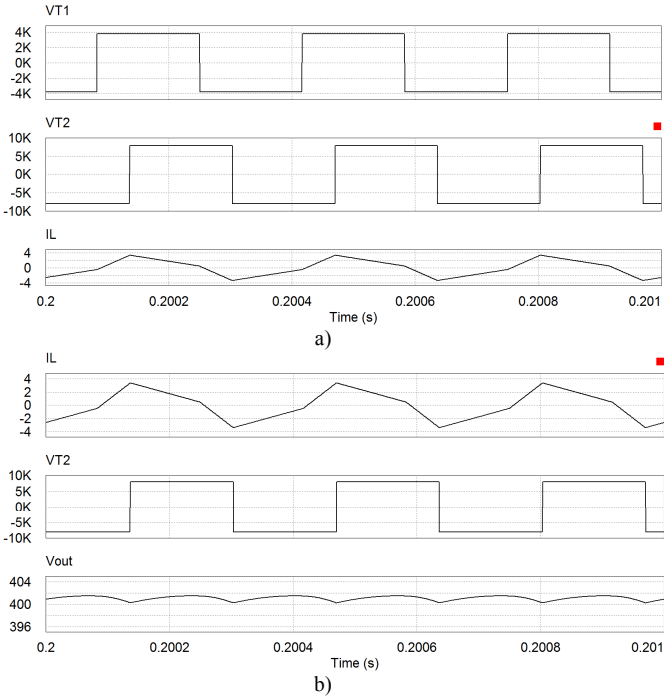

Fig. 5. Simulated results at steady state, in all cases from top to bottom: a) V_{T1}, V_{T2}, and Inductor current, b) Inductor current, V_{T2}, and output voltage ripple.

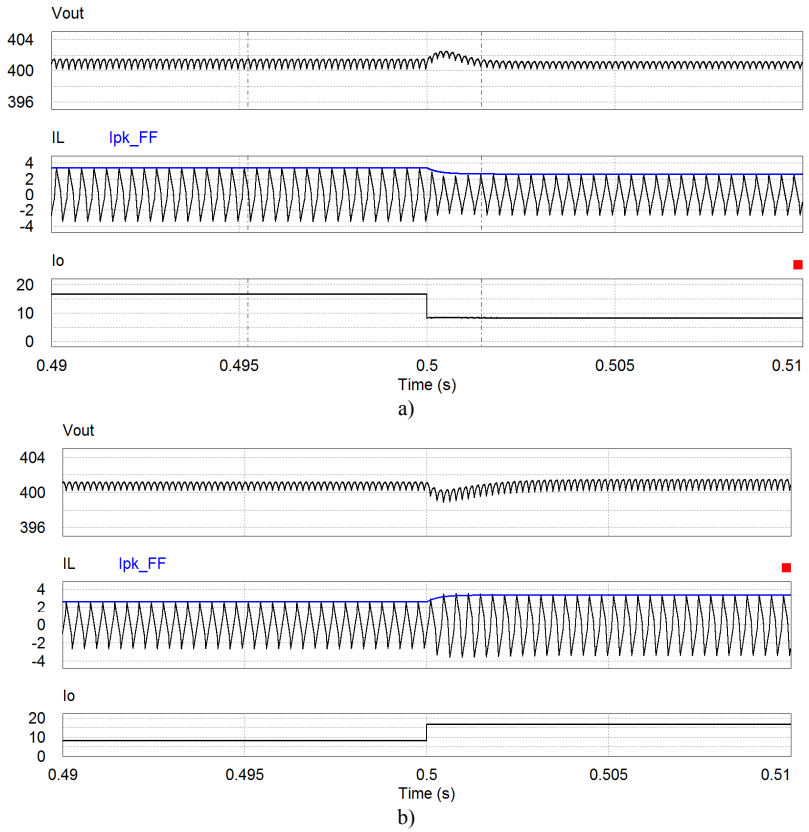

Fig. 6. Simulated results under load variation, from top to bottom: Output voltage, feed-forward compensator output ($I_{PK\text{-}FF}$), inductor current, and output current. a) load reduction, b) load increment.

TABLE I. SYSTEM PARAMETERS

System parameter	Value
Transformer ratio	20:1
Inductance L	165mH
Switching frequency	3kHz
V_{DC}	3.8kV
V_{OUT}	400V
P_o	7kW
R_1	24Ω
R_1	48Ω
K_P	0.25

was of 2.5V above the desired output voltage; as it can be observed a very fast dynamic response was obtained. In Fig. 6(b) is shown the load variation from 48Ω to 24Ω; again are shown the output voltage, the inductor current, the current obtained from the feed-forward compensator, but also the output current. The dynamic response obtained for this second test is satisfactory, around 20ms is the settling time.

C. *Avoiding transformer saturation*

The system was tested with a dc source voltage in series with the transformer primary winding, this permit to evaluate the performance of the system and verify properly if it is avoided the transformer saturation. The voltage source has a value of 1V. Fig. 7 illustrates the operation under this circumstance, the output voltage, the inductor current, and output current are shown.

As it can be observed in Fig. 7(a) the inductor current shows at the beginning that is becoming negative, and this is because at the start-up the controller is not working, since a fixed modulation is given. Once the controller is under operation, at around 110ms, the current is returned to the proper value that avoids transformer saturation.

In Fig. 7(b), a zoom at the time 110ms is shown, where the details of the inductor current are appreciated more clearly.

V. CONCLUSION

The DAB converter is used in different applications, like solid state transformers, electric vehicles, and so on. Most of the published papers are related to different modulation techniques and/or increase the efficiency of this topology. Some other works are related to the current control and some of them to avoid transformer saturation.

In this paper is proposed a double-band peak current controller with a feed-forward compensation. The proposal permits to have a very fast dynamic response under load variations but also avoids effectively the transformer saturation.

The system was described, analyzed, and numerically simulated; different tests were performed to show clear evidence that the proposal is suitable with a fast dynamic

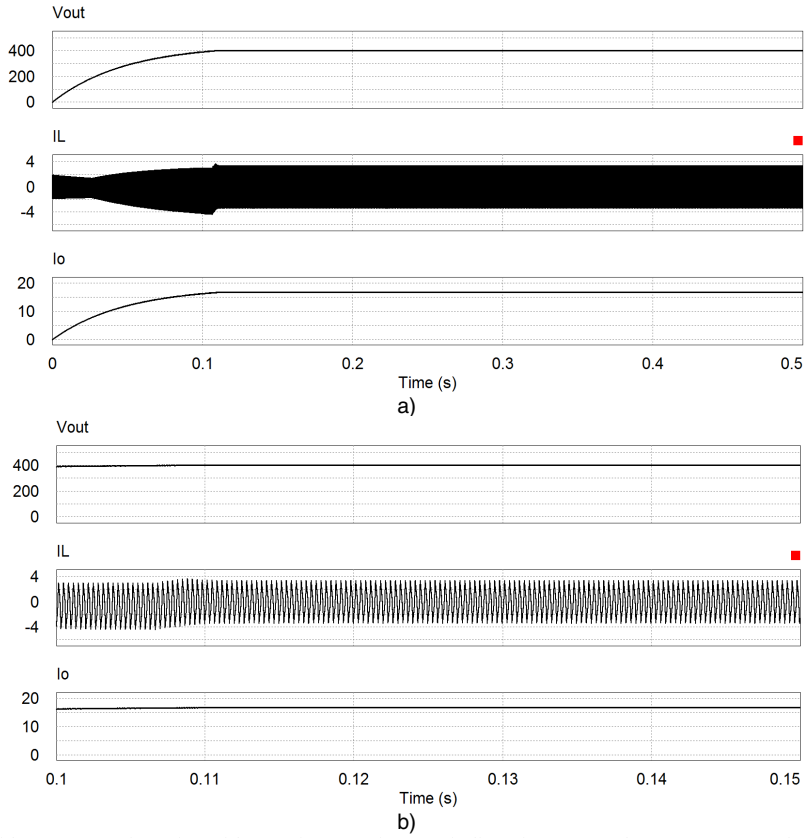

Fig. 7. Simulated results with DC source in series with transformer primary winding, from top to bottom: Output voltage, inductor current, and output current. a) Complete evolution, b) zoom.

response, but also permits to prevent the transformer saturation.

REFERENCES

[1] T. Zhao, G. Wang, J. Zeng, S. Dutta, S. Bhattacharya, and A.Q. Huang, "Voltage and power balance control for a cascaded multilevel solid state transformer," In IEEE *Applied Power Electronics Conference and Exposition (APEC)*, Feb. 2010, pp. 761-767.

[2] J. Shi, W. Gou, H. Yuan, T. Zhao, and A.Q. Huang, "Research on voltage and power balance control for cascaded modular solid-state transformer," *IEEE Trans. on Power Electron.*, vol. 26, no. 4, April 2011, pp. 1154-1166.

[3] X. She, A.G. Huang, S. Lukic, and M.E. Baran, "On integration of solid-state transformer with zonal DC microgrid," *IEEE Trans. on Smart Grid*, vol. 3, no. 2, June 2012, pp. 975-985.

[4] H. Qin, and J.W. Kimball, "Solid-state transformer architecture using AC–AC dual-active-bridge converter," *IEEE Trans. on Ind. Electron.*, vol. 60, no. 9, Sept. 2013, pp. 3720-3730.

[5] T. Zhao, G. Wang, S. Bhattacharya, and A.G. Huang, "Voltage and power balance control for a cascaded H-bridge converter-based solid-state transformer," *IEEE Trans. on Power Electron.*, vol 28, no. 4, April 2013, pp. 1523-1532.

[6] M. Liserre, G. Buticchi, M. Andresen, G. De Carne, L.F. Costa, and Z.X. Zou, "The smart transformer: Impact on the electric grid and technology challenges," *IEEE Ind. Electron. Magazine*, vol 10, no. 2, June 2016, pp. 46-58.

[7] L. Costa, G. Buticchi, and M. Liserre, "Optimum Design of a Multiple-Active-Bridge DC-DC Converter for Smart Transformer," *IEEE Transactions on Power Electronics*. Early access 2018.

[8] B.J. Vermulst, J.L. Duarte, C.G. Wijnands, and E.A. Lomonova, "Quad-Active-Bridge Single-Stage Bidirectional Three-Phase AC–DC Converter With Isolation: Introduction and Optimized Modulation," *IEEE Trans. on Power Electron.*, vol 32, no. 4, April 2017, pp. 2546-2557.

[9] L.F. Costa, L. G. Buticchi, and M. Liserre, "Quad-Active-Bridge DC–DC Converter as Cross-Link for Medium-Voltage Modular Inverters," *IEEE Trans. on Ind. Appl.*, vol. 53, no. 2, march/april 2017, pp 1243-1253.

[10] G. Buticchi, M. Andresen, M. Wutti, and M Liserre, "Lifetime-based power routing of a quadruple active bridge DC/DC converter," *IEEE Trans. on Power Electron.*, vol. 32, no. 11, Nov. 2017, pp. 8892-8903.

[11] R. Zhu, G. De Carne, F. Deng, and M. Liserre, "Integration of large photovoltaic and wind system by means of smart transformer," *IEEE Trans. on Ind. Electron.*, vol. 64, no. 11, nov. 2017, pp. 8928-8938.

[12] G. Buticchi, L.F. Costa, D. Barater, M. Liserre, and E. Dominguez, "A Quadruple Active Bridge Converter for the Storage Integration on the More Electric Aircraft," *IEEE Trans. on Power Electron.* Early access 2018.

[13] F. Krismer, and J.W. Kolar,. "Accurate power loss model derivation of a high-current dual active bridge converter for an automotive application," *IEEE Trans. on Ind. Electron.*, vol. *57,* no. 3, March 2010, pp. 881-891.

[14] Y. Shi, R. Li, Y. Xue, and H. Li, "Optimized operation of current-fed dual active bridge DC–DC converter for PV applications," *IEEE Trans. on Ind. Electron.*, vol. 62, no. 11, Nov. 2015, pp. 6986-6995.

[15] G.G. Oggier, G.O. Garcia, and A.R. Oliva, "Switching control strategy to minimize dual active bridge converter losses," *IEEE Trans. on Power Electron.,* vol. 24, no. 7, July 2009, pp. 1826-1838.

[16] G.G. Oggier, G.O. Garcia, and A.R. Oliva, "Modulation strategy to operate the dual active bridge DC–DC converter under soft switching in the whole operating range," *IEEE Trans. on Power Electron.*, vol. 26, no. 4, April 2011, pp. 1228-1236.

[17] G.G. Oggier and M. Ordonez, "High-efficiency DAB converter using switching sequences and burst mode," *IEEE Trans. on Power Electron.*, vol. 31, no. 3, March 2015, pp. 2069-2082.

[18] L.F Costa, G. Buticchi, and M. Liserre, "Highly Efficient and Reliable SiC-Based DC–DC Converter for Smart Transformer," *IEEE Trans. on Ind. Electron*., vol. 64, no. 10, Oct. 2017, pp. 8383-8392.

[19] S. Han, I. Munuswamy, and D. Divan, "Preventing transformer saturation in bi-directional dual active bridge buck-boost DC/DC converters," IEEE *Energy Conversion Congress and Exposition (ECCE), Sept. 2010 IEEE,* pp. 1450-1457.

[20] S. Dutta, S. Hazra, and S. Bhattacharya, "A digital predictive current-mode controller for a single-phase high-frequency transformer-isolated dual-active bridge DC-to-DC converter," *IEEE Trans. on Ind. Electron.*, vol. 63, no. 9, Sept. 2016, pp. 5943-5952.

[21] J. Huang, Y. Wang, Z. Li, and W. Lei, "Predictive valley-peak current control of isolated bidirectional dual active bridge DC-DC converter" IEEE *Energy Conversion Congress and Exposition (ECCE), Sept. 2015,* pp. 1467-1472.

[22] R.T. Naayagi, A.J. Forsyth, and R. Shuttleworth, "Bidirectional control of a dual active bridge DC–DC converter for aerospace applications," *IET Power Electron.*, vol. 5, no. 7, July 2012, pp. 1104-1118.

[23] W. Song, N. Hou, and M. Wu, "Virtual Direct Power Control Scheme of Dual Active Bridge DC–DC Converters for Fast Dynamic Response," *IEEE Trans. on Power Electron.*, vol. 33, no. 2, Feb. 2018, pp. 1750-1759.

[24] M. Nasr, S. Poshtkouhi, N. Radimov, C. Cojocaru, and O. Trescases, " Fast average current mode control of dual-active-bridge DC-DC converter using cycle-by-cycle sensing and self-calibrated digital feedforward," IEEE *Applied Power Electronics Conference and Exposition (APEC), march 2017,* pp. 1129-1133.

[25] F. Xiong, J. Wu, Z. Liu, and L. Hao, "Current Sensorless Control for Dual Active Bridge DC–DC Converter with Estimated Load-Current Feedforward," *IEEE Trans. on Power Electron.*, vol. 33, no. 4, Arpil 2018, pp. 3552-3566.

[26] F. An, W Song, B. Yu, and K. Yang, "Model Predictive Control with Power Self-balancing of the Output Parallel DAB DC-DC Converters in Power Electronic Traction Transformer," *IEEE Journal of Emerging and Selected Topics in Power Electronics*. Early access 2018.

[27] D. Segaran, D.G. Holmes, and B.P. McGrath, "Enhanced load step response for a bidirectional dc–dc converter," *IEEE Trans. on Power Electron.*, vol. 28, no.1, Jan. 2013, pp. 371-379.

[28] G.G. Oggier, M. Ordonez, J.M. Galvez, and F. Luchino, "Fast transient boundary control and steady-state operation of the dual active bridge converter using the natural switching surface," *IEEE Trans. on Power Electron.*, vol. 29, no. 2, Feb. 2014, pp. 946-957.